



## OPEN HPTLC based screening method for the evaluation of $\alpha$ -amylase inhibitory activity in edible flowers

Szymon Litewski<sup>✉</sup>, Marika Mróz & Barbara Kusznierewicz<sup>✉</sup>

This study introduces a High-Performance Thin-Layer Chromatography (HPTLC)-based method for assessing  $\alpha$ -amylase activity and inhibition. The method was designed as an alternative to the conventional 3,5-dinitrosalicylic acid (DNS) assay, which reports only total inhibition and lacks information on specific hydrolysis products. Starch hydrolysis was examined using  $\alpha$ -amylase from porcine pancreas, human saliva, and *Aspergillus oryzae*. Coupling HPTLC with mass spectrometry enabled the identification of six products formed during enzymatic breakdown. For validation, three key markers of activity (maltose, maltotriose, maltotetraose) were quantified after 30 min of incubation, confirming accuracy and reproducibility. The validated approach was applied to twelve edible flowers tested as hydroalcoholic extracts and infusions. Heather, peony, and rose showed the highest inhibitory activity, corresponding to  $7.68 \pm 0.37$ ,  $2.37 \pm 0.11$ , and  $1.77 \pm 0.07$  mg acarbose equivalents per gram of dry weight, respectively. Compared with the DNS assay, the HPTLC method demonstrated greater precision, minimized matrix interference, and, uniquely, allowed direct visualization of how inhibitors altered both total activity and the distribution of hydrolysis products. These advantages highlight the value of HPTLC as a screening tool for complex plant materials and support its potential in food research, nutraceutical development, and quality control.

**Keywords**  $\alpha$ -amylase inhibition, Starch hydrolysis products, HPTLC, DNS assay, Edible flowers

Starch is a carbohydrate that functions as a versatile raw material in diverse industrial applications and plays a fundamental role in human nutrition. As one of the most abundant plant-derived polysaccharides, global starch production exceeds 50 million tons annually<sup>1</sup>. Starch consists of two polymers: unbranched amylose and branched amylopectin with glucose units linked by  $\alpha$ -1,4- and  $\alpha$ -1,6-glycosidic bonds<sup>2,3</sup>. Enzymatic hydrolysis of starch is crucial across sectors including food, paper, bioplastics, and fermentation<sup>1,4,5</sup>. This process relies on glycoside hydrolases, mainly  $\alpha$ -amylases (EC 3.2.1.1), responsible for nonselective hydrolysis of internal  $\alpha$ -1,4-glycosidic bonds in amylose and amylopectin, producing maltose, maltotriose, and higher oligosaccharides, used in syrups, thickeners, and stabilizers<sup>3,6</sup>.

Beyond industrial significance, starch hydrolysis is critical in human nutrition, providing about 80% of global daily caloric intake<sup>1</sup>. Starch digestion begins in the mouth and continues in the small intestine, where salivary and pancreatic  $\alpha$ -amylase generate glucose, which serve as a fundamental source of energy for cellular metabolism<sup>7,8</sup>. The regulation of carbohydrate metabolism is crucial, as imbalances cause major health issues. The rate of polysaccharide hydrolysis, expressed as glycaemic index (GI), influences postprandial glycaemia and insulin secretion, both critical in type 2 diabetes (T2D) management<sup>9</sup>. With T2D affecting 589 million people in 2024 and projected to reach 853 million by 2050, glycaemic control strategies are increasingly important<sup>10,11</sup>. Chronic hyperglycaemia leads to severe complications, including organ damage, cardiovascular disease, neuropathy, and retinopathy<sup>11–14</sup>. The primary goal of antidiabetic therapy is to stabilize blood glucose and reduce insulin resistance. Current drugs and enzyme inhibitors such as acarbose often cause side effects like hypoglycaemia or gastrointestinal discomfort<sup>15</sup>. Therefore, there is a growing interest in natural sources of compounds with antidiabetic potential. Over 1,200 plant species have been reported as potential source of carbohydrate-hydrolysing enzymes inhibitors<sup>15</sup>. Plant remedies in the form of teas, capsules, or extracts are often used as complementary therapies in the treatment of T2D<sup>16</sup>. Nowadays, edible flowers are gaining popularity due to their aesthetic, nutritional value, and abundance of bioactive compounds<sup>17,18</sup>. The search for new varieties of medicinal plants as well as the verification of the effects of preparations already available on the market requires suitable methods to assess glycosidase activity.

Department of Chemistry, Technology and Biotechnology of Food, Faculty of Chemistry, Gdańsk University of Technology, GdańskNarutowicza Street 11/12, 80-233, Poland. <sup>✉</sup>email: szymon.litewski@pg.edu.pl; barbara.kusznierewicz@pg.edu.pl

Conventional methods for assessing  $\alpha$ -amylase activity are mainly based on spectrophotometric assays that detect changes in the total concentration of reducing sugars, e.g., 3,5-dinitrosalicylic acid (DNS), iodine-starch, and chromogenic tests<sup>19</sup>. However, these methods are prone to interference from reducing substances and overlapping absorption spectra in the complex reaction mixtures containing plant metabolites. Notably, the DNS assay was recently standardized within the INFOGEST network, improving reproducibility, though applicability to complex food matrices remains uncertain<sup>20</sup>. Alternative chromatographic approaches offer greater precision by separating reaction products. High-performance liquid chromatography (HPLC) approach has been used for the determination of inhibition and activity of different amylolytic enzymes since last century<sup>21</sup>. However, it poses challenges like enzyme precipitation and system clogging, causing disruptions in the results. In contrast, high-performance thin-layer chromatography (HPTLC) provides a cost-effective alternative for parallel analysis with minimal solvents. It has been applied in the quantitative determination of the total sugar or starch content in food samples<sup>22,23</sup>. However, such analyses require post-chromatographic derivatization (e.g., with diphenylaniline-phosphoric acid or ethylamine) to enable densitometric detection<sup>24,25</sup>. More recently, HPTLC was adapted to monitor amylase activity by tracking starch breakdown. Müller & Morlock (2024)<sup>26</sup> performed enzymatic hydrolysis reaction directly on the surface of a TLC plate, which later was also applied to evaluate the  $\alpha$ -amylase inhibitory activity of different types of flour<sup>27</sup>. However, maintaining on-surface reactions proved challenging, which may impact the obtained results. An alternative was proposed by Litewski et al. (2023)<sup>28</sup>, performing hydrolysis in aqueous solution before HPTLC separation.

This study applies and validates an HPTLC-based procedure to measure  $\alpha$ -amylase activity and inhibition. Unlike spectrophotometric assays, the method enables direct visualization of hydrolysis products and reveals how natural inhibitors alter the reaction profile. A particular strength of this method is the ability to analyze multiple samples simultaneously under identical conditions, providing rapid and reproducible comparisons that are difficult to achieve with colorimetric tests such as the DNS assay. The novelty lies in extending HPTLC beyond activity measurement: comparing hydrolysis profiles from different  $\alpha$ -amylases sources, identifying main products by HPTLC coupled with mass spectrometry (MS), and validating quantitative markers. The method was then applied as a screening tool to assess inhibitory potential of infusions and hydroalcoholic extracts of 12 commercially available edible flowers. For most species, such activity was reported for the first time. Most importantly, our results demonstrate that HPTLC not only provides accuracy and reproducibility comparable to the DNS assay, but also offers unique insights by showing the direct effect of inhibitors on starch hydrolysis profiles. To the best of our knowledge, this concept has not previously been proposed for the preliminary assessment of the antidiabetic potential of plant extracts. With ongoing advances in hyphenated HPTLC techniques, the proposed method offers an innovative tool for screening natural inhibitors and supports future applications in food research, nutraceuticals, and functional food design for diabetes management.

## Results and discussion

### Comparative analysis of $\alpha$ -amylase from different origins

The source organism of commercially available  $\alpha$ -amylases influences their substrate specificity, optimal conditions, and the composition of hydrolysis products. Depending on their origin,  $\alpha$ -amylases may produce yield different ratios of maltose, glucose, or dextrans. The screening method for  $\alpha$ -amylase activity should enable straightforward measurement, particularly by generating hydrolysis products that can be easily separated and quantified by HPTLC, without interference from plant extract components. For this reason, in the first stage of the study, the profiles of starch hydrolysis products formed by the action of three types of  $\alpha$ -amylases were compared: human saliva  $\alpha$ -amylase (HA), porcine pancreas  $\alpha$ -amylase (PA) and *Aspergillus oryzae*  $\alpha$ -amylase (AA). The concentrations of the tested enzymes in the reaction mixtures were determined spectrophotometrically to ensure equal initial activity (0.6 U/mL). Enzymatic digestion of starch was carried out in aqueous conditions for 5, 10, 20, 30, and 45 min in 37 °C in test tubes to ensure optimal and consistent reaction conditions. The obtained post-reaction mixtures were analysed by both spectrophotometric and HPTLC methods. The obtained results are presented in Fig. 1.

For spectrophotometric analysis, the DNS method was used to determine starch hydrolysis products. DNS test is commonly used to determine reducing sugars such as glucose, maltose and lactose. It is based on the reduction of 3,5-dinitrosalicylic acid by carbonyl groups of sugars, leading to the formation of a coloured complex, the intensity of which correlates with the concentration of reducing sugars in the sample<sup>29</sup>. The results presented in Fig. 1D indicate a linear increase in the concentration of reducing sugars over 45 min of starch digestion with three different  $\alpha$ -amylases. For HA and PA, the changes in colour of the reaction mixtures remained comparable over time. Statistical analysis of the reaction rates ( $\Delta$ Abs/min) revealed no significant difference between HA and PA (Student's t-test,  $p=0.374$ ). A slightly different pattern was observed in the case of AA, for which the manufacturer declared the addition of lactose as an enzyme stabiliser. The presence of this additional reducing sugar in the mixture generated high background absorbance, making measurement of starch digestion products difficult, thus the reaction rate of AA differed significantly ( $p<0.0001$ ) from both HA and PA. Nevertheless, time-dependent absorbance profiles obtained with the DNS assay were highly consistent across enzymes, as indicated by Pearson's correlation analysis ( $r=0.99$ ) for all pairwise comparisons.

In the HPTLC method, the starch hydrolysis products are separated on the plate and then visualized using a diphenylamine reagent in a phosphoric acid medium. The obtained profiles with blue bands visible in white light (Fig. 1A) were quantified densitometrically at 625 nm (Fig. 1B), which is one of the absorbance maxima characteristics of glucose and its oligomers. The integrated peak areas of starch hydrolysis products are shown in Fig. 1C. Starch digestion with HA and PA showed a similar sum of products after 45 min, but their profiles and formation dynamics differed slightly. For PA, the main product was compound "a" ( $R_f=0.32$ ), followed by "b" ( $R_f=0.22$ ) and "c" ( $R_f=0.15$ ). Interestingly, at the initial stage of HA hydrolysis, the dominant product was "c", followed by "b" and "a". After 30 min, their levels were equal, and after 45 min, as with PA, "a" was most

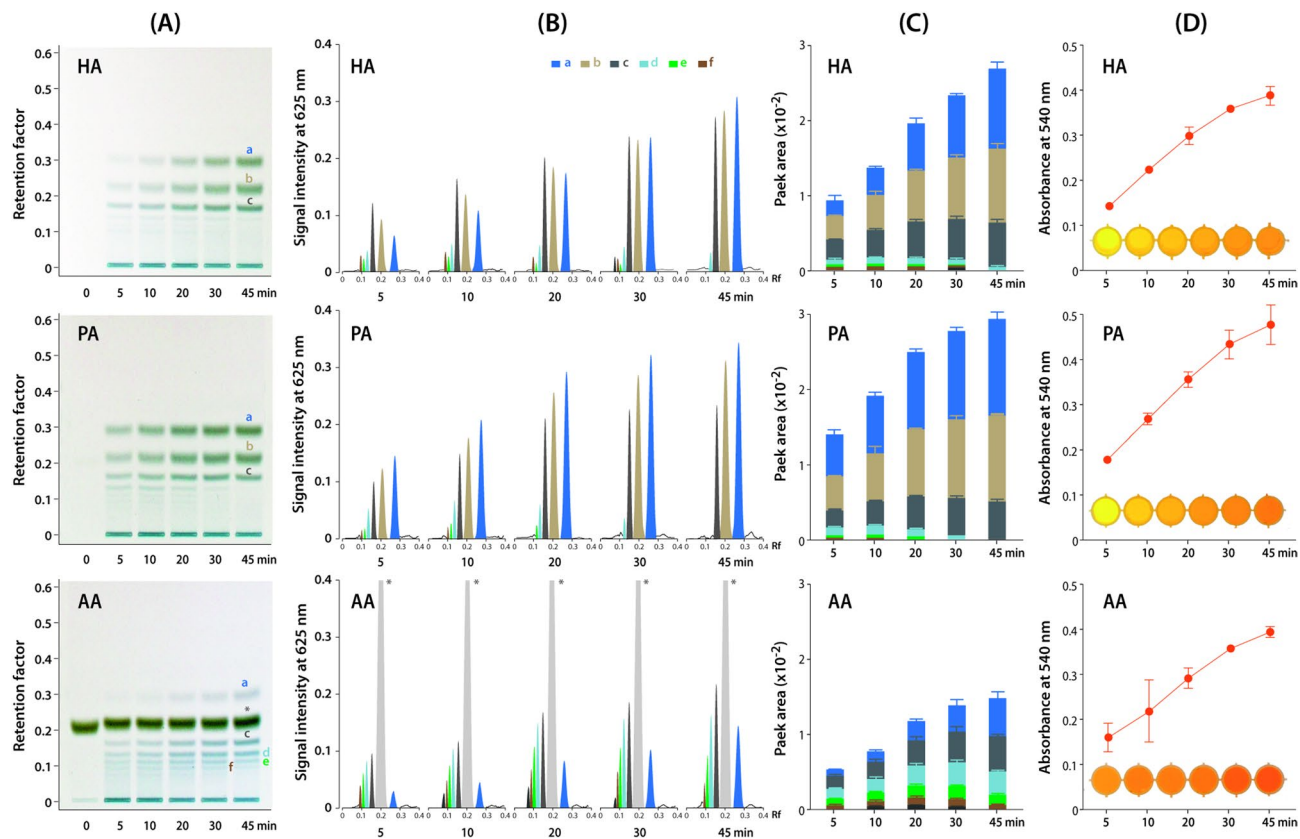


**Fig. 1.** Kinetics of starch hydrolysis by  $\alpha$ -amylase from different sources, including human saliva (HA), porcine pancreas (PA) and *Aspergillus oryzae* (AA), monitored over a time range of 0–45 min by HPTLC (A, B, C) and the DNS assay (D). Panel (A) shows HPTLC plate images recorded under white light, while panels (B) and (C) show densitograms recorded at 625 nm and the corresponding peak area values. The main products of starch hydrolysis are marked with the letters *a*, *b*, *c*, *d*, *e*, *f*, while lactose, present in the AA sample, is marked with the symbol \*. Panel (D) shows a graph of the absorbance changes of starch hydrolysis products solutions after reaction with DNS reagent, combined with photographs of these solutions.

abundant, followed by “*b*” and “*c*”. HA and PA are of mammalian origin, and their activity is mainly related to their common digestive functions, which justifies the observed similarity of starch degradation profiles. In contrast, AA being of fungal origin, exhibits different biological functions; therefore, its profile of starch digestion products was different. The main starch hydrolysis products in this case were compounds with lower  $R_f$  parameters (0.08–0.15) marked with the letters “*c*”, “*d*”, “*e*”, “*f*” (Fig. 1A). Their content increased during the reaction, but the overall product level was lower compared to the results obtained for the HA and PA enzymes. Products “*d*”, “*e*”, “*f*” were also observed at early time points in mammalian enzyme profiles, particularly in the HA. In the case of AA, a distinct band marked with “\*” was observed in the starch hydrolysis products profiles, corresponding to lactose added by the manufacturer (Fig. 1A). In conclusion, the sugar separation step using the proposed HPTLC method facilitates more effective monitoring and elimination of interfering factors, offering advantages over the DNS method. The total product amounts measured by HPTLC strongly correlated with DNS results ( $r=0.99$ ), but only HPTLC revealed product composition and enzyme-specific hydrolysis dynamics, which provides a more accurate study of enzyme kinetics and a deeper understanding of their mechanisms of action.

### Identification of the main products of starch hydrolysis by $\alpha$ -amylase

In the first stage of the study, HPTLC profiles of starch hydrolysis products revealed 3 to 6 major compounds ( $R_f$  0.08–0.32), depending on enzyme origin and reaction time. The use of HPTLC to separate mixtures of dextran oligosaccharide products was utilized by Yi et al. (2015)<sup>30</sup> to determine the action pattern of dextranase. In their studies, the bands observed in HPTLC profiles were attributed to oligosaccharides of varying degrees of polymerization (dp), separated accordingly: monosaccharides (dp 1) showed the highest  $R_f$  values, while longer oligosaccharides (up to dp 10) exhibited progressively lower  $R_f$  values. To confirm this relationship observed by Yi et al. (2015)<sup>30</sup>, the present study aimed to identify the main starch degradation products formed by mammalian and fungal  $\alpha$ -amylase. For this purpose, the obtained post-reaction mixtures containing starch and  $\alpha$ -amylase were subjected to separation on the HPTLC plate (MS-grade). Visualisation of analytes using the derivatizing reagent was performed only on a part of the developed plate. The regions corresponding to the expected  $R_f$  values of the starch degradation products bands were marked on the unsprayed part of the plate

to ensure proper alignment of the elution head. The analytes were then extracted from the silica gel by the flowing mobile phase, which was directed to the mass spectrometer with the use of TLC-MS interface (Fig. 2A). Three authentic standards (maltose, maltotriose, maltotetraose) were analysed in parallel. For these features, identities were confirmed by HPTLC co-migration ( $\Delta R_f < 0.02$ ) and MS/MS spectral matching, which we report as Level 1 (confirmed) identifications. For higher malto-oligosaccharides (dp5-dp7), authentic standards were not available; therefore, we report Level 2 (putative) annotations based on exact mass ( $\leq 5$  ppm), adduct type, and diagnostic MS/MS fragments (e.g., successive neutral losses of 162 Da and characteristic glycosidic/cross-ring cleavages).

The degree of polymerisation (dp) was assigned from accurate-mass measurements in negative-ion mode, detecting either  $[M - H]^-$  or, for lower dP,  $[M + HCOO]^-$  adducts, and supported by HRMS/MS fragmentation. Sequence information followed the Domon & Costello (1988) nomenclature<sup>31</sup> and was derived from diagnostic glycosidic and cross-ring fragments (Fig. 2B). Additionally, the fragmentation pattern of oligosaccharides and the  $MS^2$  spectra of six starch degradation products (marked as letters “a”, “b”, “c”, “d”, “e”, “f”) obtained are shown in Fig. 2B and C, respectively. Four of detected saccharides (“c”, “d”, “e”, “f”) preferably formed pseudomolecular ions  $[M - H]^-$ , while for the other two (“a”, “b”) formate adducts  $[M + HCOO]^-$  were observed. In the  $MS^2$  spectra, characteristic fragments are marked as  $A_i$ ,  $B_i$  and  $C_i$ , where “i” represents the number of the glycosidic bonds cleaved, counted from the non-reducing end. The simplest fragmentation of the carbohydrate moiety of glycoconjugates and glycosides in  $MS^2$  results from the cleavage of the glycosidic bond, providing information regarding the sugar sequences<sup>31</sup>. These types of ions were observed in the  $MS^2$  spectra obtained in the presented study:  $B_1$  ( $m/z$  161),  $C_1$  ( $m/z$  179),  $C_2$  ( $m/z$  341),  $C_3$  ( $m/z$  503),  $B_4$  ( $m/z$  647),  $C_4$  ( $m/z$  665) and  $C_5$  ( $m/z$  827). In addition, more complex processes involving transverse fragmentation of the sugar ring were also observed and were designated as ions  $^{0,2}A_i$ ,  $^{2,4}A_i$  and  $^{2,5}A_i$ . Accordingly, the band with the highest  $R_f$  (“a”;  $R_f = 0.32$ ) was

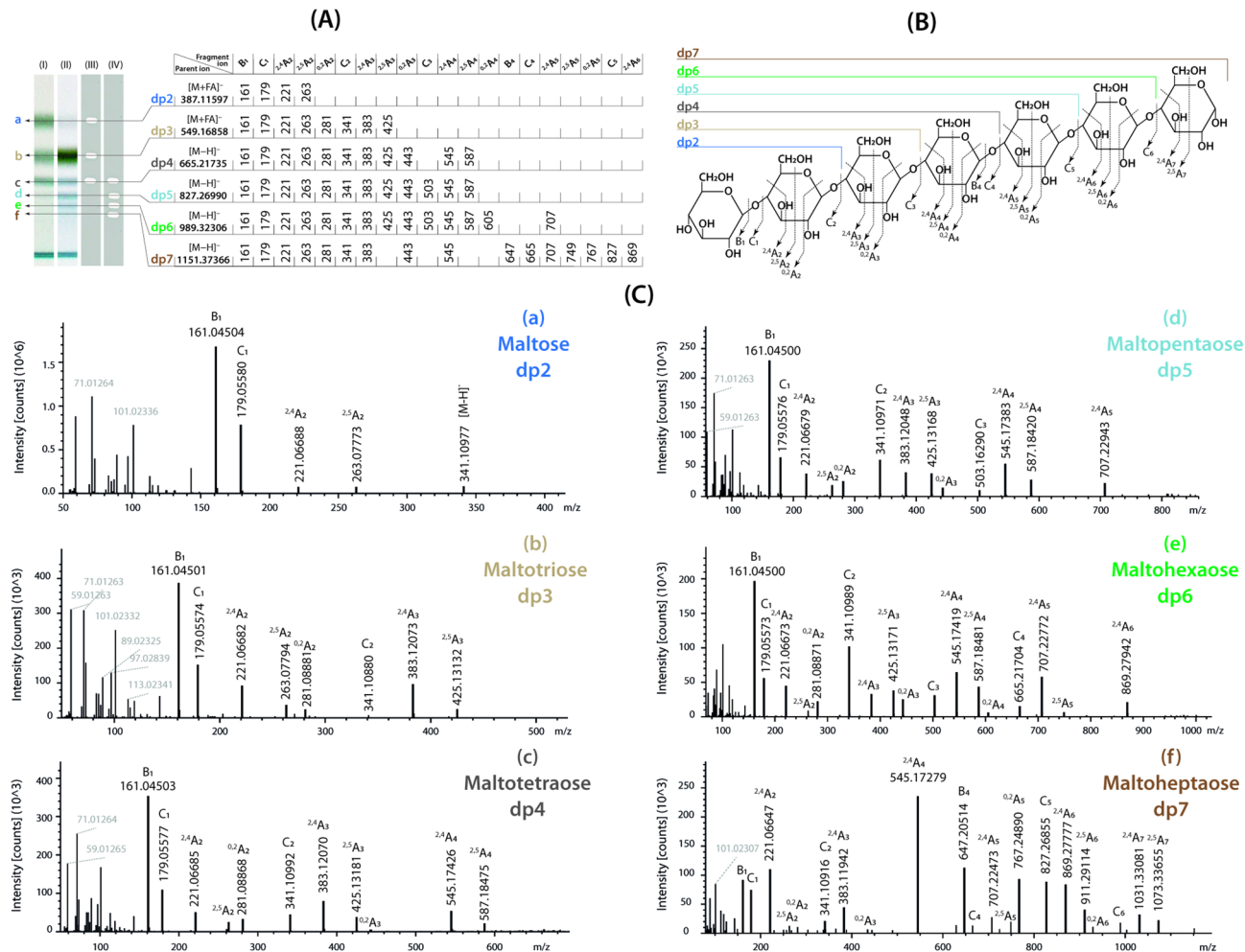


**Fig. 2.** HPTLC profiles of samples obtained from reaction of starch with porcine amylase (PA) (I, III) and *Aspergillus oryzae* amylase (AA) (II, IV) after derivatization (I, II) and without derivatization (III, IV) used during isolation and identification of starch degradation products with assignment of molecular ions and fragment ions (A) combined with the fragmentation pattern of oligosaccharides (B) and  $MS^2$  fragmentation spectra of six starch degradation products (marked as letters “a”, “b”, “c”, “d”, “e”, “f”) obtained in the negative ion mode (C).

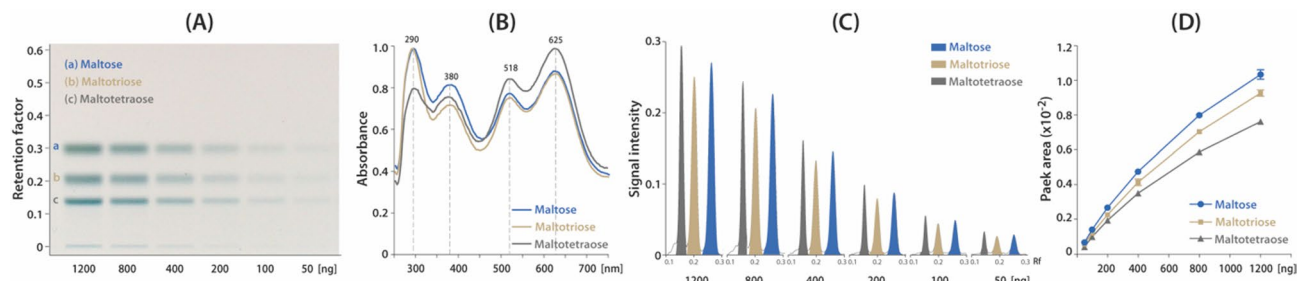


**Fig. 3.** Results of the validation of the HPTLC method using maltose, maltotriose and maltotetraose as standards. Panel (A) shows HPTLC chromatograms of mixtures of standards at different concentrations, derivatized and recorded under white light. Panel (B) shows UV-Vis spectra generated from the plate after derivatization of the standards, while panels (C) and (D) show densitograms recorded at 625 nm and corresponding calibration curves, respectively.

Compound	Linearity and detectability (50–800 ng/band)					Accuracy (400, 600, 800 ng/band)		Precision (400 ng/band)	
	Regression equation	Coefficient of determination ( $R^2$ )	LOD [ng]	LOQ [ng]	Mean % recovery $\pm SD$ ( $n=9$ )	RSD%	Intra-day %RSD ( $n=7$ )	Inter-day %RSD ( $n=9$ )	
Maltose	$y = 9.6E-06x + 0.0008$	0.990	$11.23 \pm 0.09$	$34.04 \pm 0.29$	$111.52 \pm 11.27$	10.11	5.80	6.60	
Maltotriose	$y = 8.5E-06x + 0.0007$	0.991	$17.07 \pm 0.19$	$51.71 \pm 0.59$	$90.32 \pm 5.44$	6.02	10.68	7.79	
Maltotetraose	$y = 7.1E-06x + 0.0007$	0.987	$13.84 \pm 0.26$	$41.49 \pm 0.79$	$96.38 \pm 5.07$	5.26	8.19	8.53	

**Table 1.** Validation parameters determined for the HPTLC method including linearity, accuracy, intra-day and inter-day precision for maltose, maltotriose and maltotetraose.

confirmed as maltose (dp2), while the next two zones were confirmed as maltotriose (“b”;  $R_f = 0.22$ , dp3) and maltotetraose (“c”;  $R_f = 0.15$ , dp4). Additional bands were putatively annotated as maltopentaose (“d”;  $R_f = 0.12$ , dp5), maltohexaose (“e”;  $R_f = 0.10$ , dp6) and maltoheptaose (“f”;  $R_f = 0.08$ , dp7).

Structural identification of these oligosaccharides enabled interpretation of enzyme-specific hydrolysis patterns. For mammalian  $\alpha$ -amylases (HA, PA), the dominant products after 45 min were maltose, maltotriose, and maltotetraose, consistent with known activity targeting linear amylose/amylopectin chains<sup>32</sup>. The similar profiles of HA and PA reflect their shared mammalian origin and digestive function. By contrast, fungal *Aspergillus*  $\alpha$ -amylase (AA) produced more diverse oligosaccharides, including maltotetraose, maltopentaose, and maltohexaose, indicating different substrate specificity and hydrolysis behaviour. Similar observations were made by Sahnoun et al. (2012)<sup>33</sup> during their investigation of two  $\alpha$ -amylase isoforms isolated from a newly identified *Aspergillus oryzae* strain S2. It was reported that those enzymes generate significant amounts of longer maltooligosaccharides at early reaction stages, with maltose and maltotriose appearing only after extended hydrolysis (up to 24 h).

Based on the results obtained in this study, PA was selected for further investigation due to its superior activity and distinct starch hydrolysis pattern. For screening assays, an optimal reaction time of 30 min was established, with maltose, maltotriose, and maltotetraose selected as markers for enzyme activity.

#### Method validation for determination of maltose, maltotriose and maltotetraose

The HPTLC method for quantifying maltose, maltotriose and maltotetraose, which were selected as markers of  $\alpha$ -amylase activity, was validated according to the ICH Q2(R1) guidelines<sup>34</sup>, assessing linearity, detectability, accuracy and precision. Chromatograms of standard mixtures (Fig. 3A) confirmed clear separation and the colour intensity of the bands varies in a dose-dependent manner. After derivatization, all standards exhibited similar UV-Vis spectra with absorbance maxima at 290, 380, 518, and 625 nm (Fig. 3B). The wavelength of 625 nm was chosen for densitometric quantification due to the highest signal intensity and the lowest probability of interference from phytochemicals present in real samples. Densitograms and corresponding calibration curves generated from three independent repetitions (Fig. 3C and D) demonstrated linearity across 50–800 ng/band, with strong correlations:  $R^2 = 0.990$  (maltose), 0.991 (maltotriose), and 0.987 (maltotetraose). Regression equations are presented in Table 1. Calibration based on peak area versus concentration was chosen as it provides consistent and accurate results across the entire calibration range, as described in the findings of Mello dos Santos (2023)<sup>35</sup>.

Detectability was assessed by calculating the limits of detection (LOD) and quantification (LOQ). Maltose exhibited the lowest LOD ( $11.23 \pm 0.09$  ng/band) and LOQ ( $34.04 \pm 0.29$  ng/band), followed by maltotetraose (LOD,  $13.84 \pm 0.26$  ng/band; LOQ,  $41.49 \pm 0.79$  ng/band) and maltotriose (LOD,  $17.07 \pm 0.19$  ng/band; LOQ,  $51.71 \pm 0.59$  ng/band), reflecting the method’s capability to detect and quantify low analyte concentrations.

Notably, for on-plate starch hydrolysis methods, the LOD values for maltose and maltotriose were determined by Müller & Morlock (2024)<sup>26</sup> to be 38 ng/band and 47 ng/band, respectively, which is about 3 times higher than the values obtained using the presented method. This increased detectability likely results from the use of diphenylamine as a derivatization reagent, which is more responsive to long-chain sugars than *p*-benzoic acid<sup>26</sup>.

Accuracy was confirmed by recovery tests at three concentration levels (400, 600, 800 ng/band), yielding recoveries of  $111.5 \pm 11.3\%$  (maltose),  $90.3 \pm 5.4\%$  (maltotriose), and  $96.4 \pm 5.1\%$  (maltotetraose). Precision ranged from 5.80 to 10.68% (intra-day) and 6.60–8.53% (inter-day), confirming good reproducibility. These results indicate that the method provides reliable and accurate quantification.

In summary, the validated HPTLC method is specific, sensitive and accurate, making it a robust tool for the quantitative determination of maltose, maltotriose and maltotetraose as markers of  $\alpha$ -amylase activity in solutions after starch hydrolysis.

### Screening of edible flower samples for $\alpha$ -amylase inhibitory activity

The validated HPTLC method was applied for screening analysis of real plant samples for their ability to inhibit  $\alpha$ -amylase activity. Edible flowers have recently gained popularity as potential natural health products with various health benefits, including anti-diabetic properties. Their phytochemical profiles vary widely between and within species, leading to differences in biological activity<sup>36</sup>. For this reason, 12 commercially available dried edible flowers were selected to test the usefulness of the developed method (Fig. 4A). Two types of samples were prepared from the dried materials: infusions and hydroalcoholic (3:7 v/v) extracts, maintaining the same ratio of dry mass to the volume of the extractant used (50 mg dw/mL). The samples were prepared as infusions because this is the most popular way of consuming dried plants. Although water is the safest and cheapest green solvent, its use is limited to the extraction of mainly polar compounds. According to previous reports, adding an organic solvent to water increases the diffusivity of the solvent in the matrix and increases the extraction efficiency of bioactive substances<sup>37</sup>. For this reason, the extracts prepared using additionally ethanol (70%) were also subjected to screening analyses. This type of extractant is considered the most universal, non-toxic and easy-to-handle for plant extraction, preferred in the food and pharmaceutical industries<sup>38</sup>.

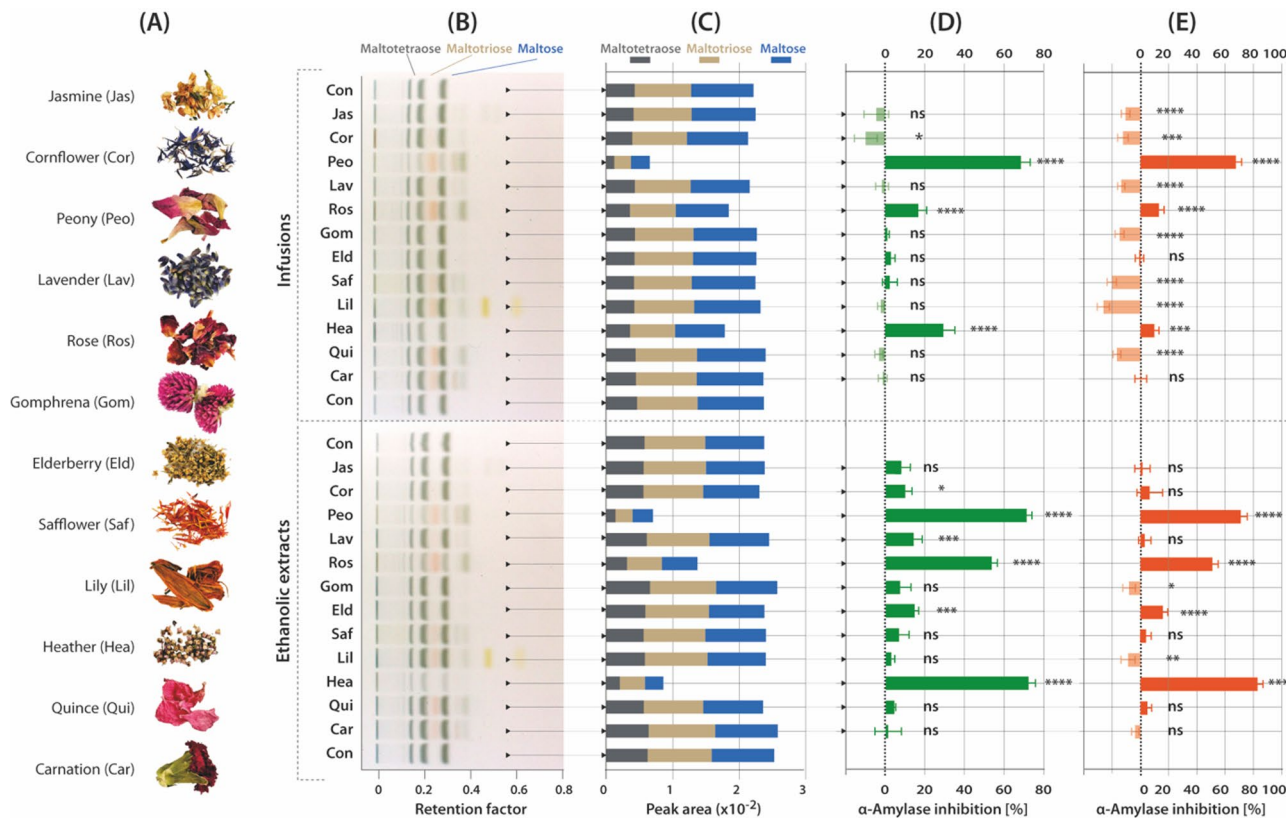


**Fig. 4.** Results of screening of edible flower infusions and hydroalcoholic extracts (70%) to determine porcine pancreatic  $\alpha$ -amylase inhibitory activity. Pictures of 12 tested flowers are presented in panel (A), while panel (B) shows HPTLC profiles of enzymatic starch hydrolysis products in mixtures without inhibitors (Con) or with tested flower samples, derivatised and recorded under white light. Panel (C) illustrates the peak areas of maltose, maltotriose and maltotetraose integrated in densitograms recorded at 625 nm.  $\alpha$ -Amylase inhibitory activity of flower extracts was calculated as % relative to the control using the HPTLC method (D) and the DNS assay (E). Results represent means  $\pm$  SD. Significantly different values determined by using one-way analysis of variance (ANOVA) with Dunnett's post-test are marked as ns - not significant; \*  $p < 0.05$ ; \*\*  $p < 0.01$ ; \*\*\*  $p < 0.001$ ; \*\*\*\*  $p < 0.0001$ .

Infusions and hydroalcoholic extracts from 12 plants were added to mixtures containing starch and PA. The reactions were stopped after 30 min and the post-reaction mixtures were analysed by HPTLC and additionally by DNS test. In HPTLC method,  $\alpha$ -amylase inhibitory activity was determined by comparing the profile of starch hydrolysis products of the mixture with the tested sample with the profile of the control sample (without inhibitors). The peak areas of three previously selected markers (maltose, maltotriose and maltotetraose) were used for quantitative determinations. Both types of flowers extracts were analysed using HPTLC method to assess chromatographic profiles, quantify bioactive markers, and evaluate  $\alpha$ -amylase inhibitory activity, with the results presented in panels B, C and D of Fig. 4, respectively. The obtained chromatographic profiles show markers of starch hydrolysis, well separated and non-coeluting with endogenous sugars present in some of the tested samples (e.g., glucose with  $R_f=0.40$  or fructose with  $R_f=0.28$ ) (Fig. 4B). In general, the content of marker saccharides for samples with hydroalcoholic extracts was lower compared to water infusions, indicating that 70% ethanol is more effective in extracting the bioactive compounds responsible for  $\alpha$ -amylase inhibition. Additionally, Student's t-test revealed no significant differences ( $p>0.999$ ) between controls containing ethanol or water, confirming that the tested ethanol concentration had no effect on  $\alpha$ -amylase activity in either the HPTLC or DNS assay. Among the flowers tested, peony (Peo) showed strong concordance between HPTLC and DNS methods, with both showing high percentage of inhibition in both water infusions (HPTLC:  $67.99\pm 4.65\%$ ; DNS:  $67.19\pm 4.16\%$ ) and hydroalcoholic extracts (HPTLC:  $70.53\pm 2.67$ ; DNS:  $70.63\pm 4.57$ ). Other samples that showed the ability to inhibit  $\alpha$ -amylase in both tests were rose (Ros) and heather (Hea) flowers ( $p<0.0001$ ). Notably, the hydroalcoholic extracts of these flowers exhibited considerable higher activity than their infusions. Discrepancies between HPTLC and DNS results were significant ( $p<0.0001$ ) for infusions with low  $\alpha$ -amylase inhibition (Lav, Gom, Saf, Lil, Hea, Qui) highlighting that the two assays diverged particularly in detecting inhibitory effects. For instance, safflower infusion showed 2.41% inhibition by HPTLC but a 20.36% increase in the DNS test. These differences may be due to the specificity of the DNS test, which is based on the reaction of the indicator with free carbonyl groups (C=O). Unfortunately, in complex matrices, this possible reaction of DNS with sample components leads to an overestimation of the sugar content due to the parallel reaction, which affects the measured absorption<sup>39</sup>. In contrast, the discrepancies between HPTLC and DNS results were significant only in the case of Hea extract ( $p=0.004$ ). Moreover, the results obtained using the DNS test for hydroalcoholic extracts showed fewer interferences, suggesting water infusions contain more compounds that distort spectrophotometric analysis.

Interestingly, most of the tested plants with low  $\alpha$ -amylase inhibitory activity (<15%) have reported antidiabetic effects for species such as jasmine, cornflower, gomphrena, elderberry, and lavender, or safflower oil<sup>40–44</sup>. This discrepancy in the results obtained in different studies may be due to differences in the analytical procedures, including extraction techniques, reaction conditions and compositions of reaction mixtures, as well as analysed plant material species, origin and morphological part. In the presented study, two independent analytical methods were used for screening tests, which provided a more solid and reliable assessment of the ability of the tested flowers to inhibit  $\alpha$ -amylase. Overall, both HPTLC and DNS assays identified peony, heather, and rose as the most potent  $\alpha$ -amylase inhibitors among the tested edible flowers.

### Determination of the $IC_{50}$ parameter of acarbose and selected plant extracts

The proposed HPTLC method allows not only to indicate samples with the highest  $\alpha$ -amylase inhibition potential but also to determine their  $IC_{50}$  parameter. For this purpose, dilution series of hydroalcoholic extracts from peony, rose, and heather, along with acarbose as a reference, were tested using both HPTLC and DNS methods (Fig. 5).

The results obtained by the HPTLC method are characterized by a smaller error and higher precision, because the measurement concerns the determination of specific markers separated from the reaction mixture (Fig. 5B). On the contrary, spectrophotometric measurement detects all products formed in the reaction of the indicator with the free carbonyl groups present in the mixture. This causes an increase in the measurement uncertainty, which is especially visible when measuring plant samples, where matrix interferences occur (Fig. 5C). Therefore, the proposed HPTLC method could serve as a more accurate alternative to conventional spectrophotometric methods for determining the  $IC_{50}$  parameter against  $\alpha$ -amylase.

The  $IC_{50}$  value for acarbose determined using the DNS test and the HPTLC method resulted in values of  $2.86\pm 0.32$  and  $4.47\pm 0.22$   $\mu$ g/mL, respectively. The higher  $IC_{50}$  value obtained by DNS assay can be attributed to methodological differences, as the HPTLC approach focuses on specific oligosaccharides (maltose, maltotriose, maltotetraose), potentially omitting part of the hydrolysis profile. However, it should be emphasized that these results refer to the same post-reaction mixture. Notably, the relative standard deviation (RSD) was lower for the HPTLC method (4.82%) compared to the DNS test (11.09%). A similar trend was observed for plant samples, where  $IC_{50}$  values obtained by the DNS method showed RSDs ranging from 9.07% to 26.75%, while the HPTLC method yielded RSDs between 3.99% and 4.75%, indicating that the HPTLC method provides a more reliable determination of  $IC_{50}$  values.

Among the flower samples tested, heather was the strongest  $\alpha$ -amylase inhibitor, followed by peony and rose. While expressing the relative  $\alpha$ -amylase inhibitory activity of these plant extracts as mg of acarbose equivalent per gram of dry plant weight (AE mg/g dw), the results obtained were  $6.57\pm 0.60$ ,  $2.10\pm 0.53$ , and  $1.10\pm 0.13$  AE mg/g dw in the DNS test, and  $7.68\pm 0.37$ ,  $2.37\pm 0.11$ , and  $1.77\pm 0.07$  AE mg/g dw in the HPTLC method. The consistency of results for these three plants across both methods underlines the reliability of the measurements. Statistical analysis using Tukey's test showed significant differences between the plants: Peo vs. Ros ( $p=0.0313$ ), Peo vs. Hea ( $p<0.0001$ ), and Ros vs. Hea ( $p<0.0001$ ), confirming that the observed variations in  $\alpha$ -amylase inhibitory activity among the extracts are statistically meaningful.

The high activity observed in the case of heather suggests that it is a richer source of  $\alpha$ -amylase-inhibiting compounds compared to peony and rose. Such activity may result from the abundance of flavonoids, which

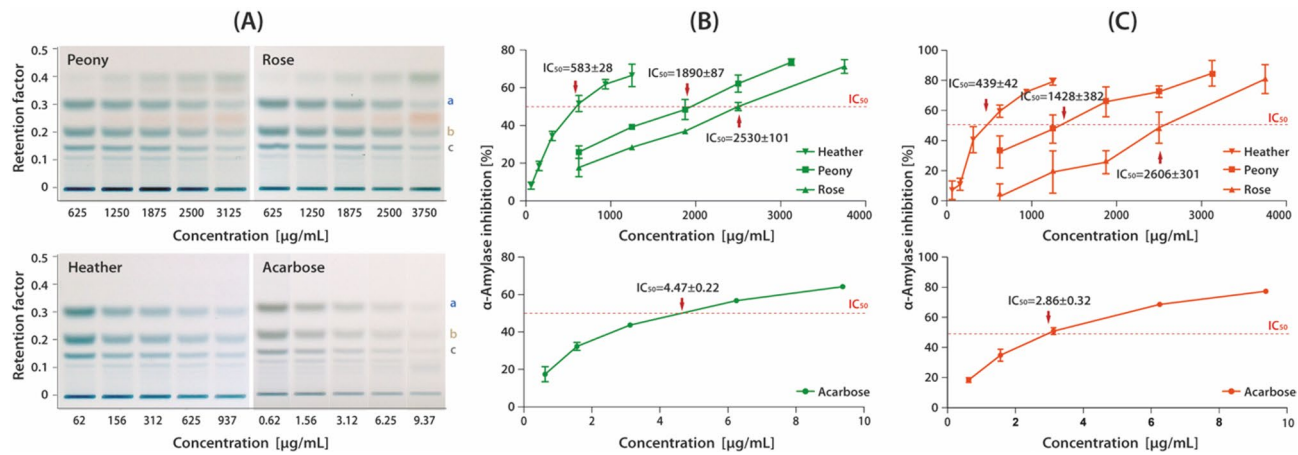


**Fig. 5.** HPTLC profiles of starch hydrolysis products - maltose (a), maltotriose (b), maltotetraose (c) - resulting from the enzymatic activity of  $\alpha$ -amylase in the presence of flower extracts with varying dry matter contents of peony, rose, heather and acarbose (A) juxtaposed with the plots of concentration- $\alpha$ -amylase inhibitory activity dependence (%) used for the determination of IC<sub>50</sub> using the HPTLC method (B) and DNS assay (C).

structural features are closely related to the enzyme-inhibiting potential due to binding to the active sites and blocking interactions with substrates<sup>7</sup>. Heather (*Calluna vulgaris*) is considered an invasive plant, but it was traditionally used as medicinal plant with a broad pharmacological potential, including antibacterial, neuroprotective, antioxidant, anti-inflammatory, and chemoprotective effects. Its bioactivity is often associated with the presence of flavonoids (mostly kaempferol derivatives), tannins, hydroxycinnamic acids, and triterpenoids (ursolic acid)<sup>45</sup>. However, further studies are needed to confirm which compounds are responsible for its  $\alpha$ -amylase inhibitory activity.

To the best of our knowledge, *Paeonia officinalis* flowers have not been previously studied for  $\alpha$ -amylase inhibition, but leaf extracts showed IC<sub>50</sub> values of 1.67–2.52 mg/mL<sup>46</sup> while *P. lactiflora* seeds showed antidiabetic potential via stilbene-mediated inhibition of PTP1B and  $\alpha$ -glucosidase<sup>47</sup>.

The weakest  $\alpha$ -amylase inhibitor among the three most promising extracts tested was the rose flowers extract, which was found to be about five times weaker than the heather extract. In the study by Simin et al. (2024)<sup>48</sup> methanol extracts from petals of new genotypes of garden roses (*Rosa x hybrida*) inhibited  $\alpha$ -amylase, depending on the genotype tested, in the range from 7.3 to 113 AE mg/g dw. Other studies have shown that adding 0.1% *Rosa rugosa* extract to yogurt significantly increased the inhibition of  $\alpha$ -amylase and  $\alpha$ -glucosidase compared to regular yogurt, while increasing sensory appeal<sup>49</sup>.

This study demonstrates that the HPTLC method provides a reliable and precise tool for screening  $\alpha$ -amylase inhibitory activity across multiple plant samples. It allows rapid identification of promising natural inhibitors, which can then be prioritized for further detailed analysis, including compound isolation, bioavailability, stability, and safety evaluation, which is essential for their potential use in supporting diabetes therapy.

## Conclusions

This work presents the development of a new analytical approach for the determination of  $\alpha$ -amylase activity by monitoring HPTLC profiles of starch degradation products based on their densitograms recorded after derivatization with diphenylamine reagent. Unlike traditional spectrophotometric assays such as DNS, this method provides chromatographic separation, enabling tracking of individual starch hydrolysis products and reducing matrix interference.

Both methods showed similar enzyme activity levels, but only HPTLC distinguished differences between mammalian and fungal  $\alpha$ -amylases. The hyphenated TLC-MS approach identified six main starch degradation products (dp2-dp7), with maltose, maltotriose, and maltotetraose used as activity markers for validation. The method's usefulness for detecting natural  $\alpha$ -amylase inhibitors was verified on water infusions and hydroalcoholic extracts of 12 edible flowers, highlighting peony, red rose, and heather as the strongest inhibitors. HPTLC also enabled comparison with the commercial inhibitor acarbose via IC<sub>50</sub> values. This approach has broad potential applications, including functional food production, nutrigenomic studies, enzyme monitoring, fermentation optimization, and  $\alpha$ -amylase inhibitor research for type 2 diabetes therapy.

## Materials and methods

### Materials and chemicals

The following chemicals and reagents were purchased from Merck KGaA (Darmstadt, Germany):  $\alpha$ -amylase from porcine pancreas (Type VI,  $\geq 5$  units/mg solid),  $\alpha$ -amylase from human salvia (Type XIII-A, lyophilized powder, 300–1,500 units/mg protein)  $\alpha$ -amylase from *Aspergillus oryzae* (lyophilised powder,  $\sim 1.5$  U/mg), boric acid, diphenylaniline, aniline, phosphoric acid, 3,5-dinitrosalicylic acid (DNS), maltose (63418), maltotetraose (M8253), acarbose (PHR1253), phosphate-buffered saline (PBS), acetonitrile (MS grade), methanol (MS grade),

ethanol, HPTLC silica gel 60 F254 plates. Soluble starch (789820118), maltotriose (63430), 2-propanol, 1-butanol, sodium hydroxide, sodium tartrate tetrahydrate were purchased from Avantor Performance Materials Poland S.A. (Gliwice, Poland). Water was purified with a QPLUS185 system from Millipore (Burlington, MA, USA) at Gdańsk University of Technology.

### Plant material and extraction

The research material consisted of 12 commercially available dried edible flowers obtained from a supplier. Ten of them were distributed by Planteon (Żelazków, Poland) including jasmine (Jas: *Jasminum officinale*), cornflower (Cor: *Centaurea cyanus*), peony (Peo: *Paeonia officinalis*), lavender (Lav: *Lavandula angustifolia*), red rose (Ros: *Rosa spp.*), gomphrena (Gom: *Gomphrena globosa*), safflower (Saf: *Carthamus tinctorius*), orange lilies (Lil: *Lilium spp.*), heather (Hea: *Calluna vulgaris*) and carnation (Car: *Dianthus caryophyllus*). Elderberry dried flowers (Eld: *Sambucus nigra*) were produced by NANGA (Poland). Japanese quince (Qui: *Chaenomeles x superba*) flowers were collected from a local plantation in Straszyn (Gdańsk, Poland), established with original seedlings from a professional nursery. All flower samples were freeze-dried, and ground using a mill. For the screening analysis of  $\alpha$ -amylase inhibitory activity, flower extracts with final concentration of 50 mg dry weight of plant per 1 mL of solvent were prepared using two different methods. Firstly, infusions were prepared by mixing 1 g of floral plant material with 20 mL of boiling distilled water. The mixture was allowed to steep for 20 min. To prepare hydroalcoholic extracts, 250 mg of plant material was suspended in 5 mL of aqueous ethanol solution (3:7 v/v). The resulting suspensions were mixed and sonicated for 30 min. After extraction water infusions and hydroalcoholic extracts were centrifuged at 4,696 x g for 15 min. The supernatants were collected and centrifuged again at 16,100 rcf for another 15 min. The final supernatants were collected and stored at  $-20^{\circ}\text{C}$  until analysis.

### Enzymatic reaction

The in-vial enzymatic reaction was performed as described by Litewski et al. (2023)<sup>28</sup> with slight modifications. The substrate solution was prepared by dissolving 250 mg of soluble starch in 10 mL of cold distilled water, followed by adding 40 mL of boiling distilled water. Enzyme solutions were prepared in PBS so that the concentrations of  $\alpha$ -amylase from human saliva (HA), porcine pancreas (PA) and *A. oryzae* (AA) had the same enzymatic activity (0.6 U/ml). This corresponded to concentrations of  $0.012 \pm 0.001$  mg/mL,  $0.078 \pm 0.003$  mg/mL, and  $6.11 \pm 0.16$  mg/mL, respectively, determined experimentally using the DNS spectrophotometric assay.

For kinetic analysis, the reaction mixture consisting of 300  $\mu\text{L}$  of PBS, 100  $\mu\text{L}$  of 70% ethanol and 800  $\mu\text{L}$  of soluble starch solution was pre-incubated in  $37^{\circ}\text{C}$  for 5 min. Then, 400  $\mu\text{L}$  of  $\alpha$ -amylase (HA, PA or AA) was added, followed by the incubation in  $37^{\circ}\text{C}$  for 5, 10, 20, 30 and 45 min. After that time, the samples were placed in a thermoblock, heated to  $100^{\circ}\text{C}$  for 5 min to stop the enzymatic reaction and immediately cooled in ice.

Later, the ability of plant extracts to inhibit activity of  $\alpha$ -amylase (PA) and the  $\text{IC}_{50}$  values of selected samples were determined in the same manner with minor modifications.  $\alpha$ -Amylase inhibitory activity was determined for all infusions and hydroalcoholic extracts. However,  $\text{IC}_{50}$  parameters were determined only for three, most prominent aqueous-ethanol extracts (Peo, Ros, Hea) and the synthetic inhibitor - acarbose. The samples were diluted with 70% ethanol: Peo and Ros extracts (625–3750  $\mu\text{g}$  dw/mL), Hea extract (60–1000  $\mu\text{g}$  dw/mL), and acarbose (0.62–10  $\mu\text{g}$  dw/mL). The composition of the reaction mixture for water infusions was as follows: 800  $\mu\text{L}$  of starch solution, 230  $\mu\text{L}$  of PBS, 70  $\mu\text{L}$  of ethanol, 100  $\mu\text{L}$  of flower infusion. The reaction mixtures for hydroalcoholic extracts contained: 800  $\mu\text{L}$  of starch solution, 300  $\mu\text{L}$  of PBS, 100  $\mu\text{L}$  of 70% hydroalcoholic flower extract. Reaction mixtures were pre-incubated at  $37^{\circ}\text{C}$  for 5 min and then mixed with 400  $\mu\text{L}$  of PA enzyme solution. Control samples were prepared in the same way, but with 100  $\mu\text{L}$  of water or 70% ethanol instead of the plant sample. The enzymatic reaction was conducted for 30 min at  $37^{\circ}\text{C}$  followed by thermal termination. The products of enzymatic hydrolysis of starch obtained in individual experiments were determined using both spectrophotometric DNS assay and proposed HPTLC method.

### DNS assay

To determine the activity of  $\alpha$ -amylase, the DNS method described by Goncalves et al. (2010)<sup>50</sup> with slight modifications was used. DNS reagent was prepared by dissolving 12 g of sodium potassium tartrate in 8 mL of 2 M NaOH and then mixed with 20 mL of 96 mM DNS. Spectrophotometric assays were performed in heat resistant 96-well plates. Each well contained 25  $\mu\text{L}$  of post-reaction mixture and 25  $\mu\text{L}$  of DNS reagent. Plates were heated at  $105^{\circ}\text{C}$  for 10 min. After cooling the plate on ice, 250  $\mu\text{L}$  of distilled water was added to each well. The absorbance ( $A$ ) was measured at 540 nm using BioTek Synergy HT Microplate Reader spectrophotometer (Santa Clara, CA, USA). Relative  $\alpha$ -amylase activity (%RAA<sub>DNS</sub>) was calculated by following equation: %RAA<sub>DNS</sub> =  $[(A_{\text{sample}} - A_{\text{sample blank}})/(A_{\text{control}} - A_{\text{control blank}})] \times 100$ , where  $A_{\text{sample}}$  is the absorbance of the reaction mixture with the tested sample;  $A_{\text{sample blank}}$  is the absorbance of the reaction mixture with the tested sample and without enzyme;  $A_{\text{control}}$  is the absorbance of the control reaction mixture with appropriate solvent instead of the sample;  $A_{\text{control blank}}$  is the absorbance of the control reaction mixture without enzyme.  $\alpha$ -Amylase inhibitory activity (%AIA<sub>DNS</sub>) was calculated as: %AIA<sub>DNS</sub> =  $100 - \text{RAA}_{\text{DNS}}$ .

### HPTLC analyses

Profiling of the enzyme reaction products to determine  $\alpha$ -amylase activity was preformed using the CAMAG HPTLC system operated by *VisionCATS* 2.5. software (CAMAG, Muttenz, Switzerland; available at <https://camag.com/product/software/>). For each analysis, silica gel HPTLC plates (20  $\times$  10 cm, F<sub>254</sub>, Merck, Darmstadt, Germany) were pre-developed with methanol and then dried for 10 min in an air stream to remove residual solvent. The plates were then wrapped in aluminium foil and left in a desiccator overnight. The reaction mixtures (2  $\mu\text{L}$ ) were applied as 8 mm bands onto pre-washed plates by an automatic ATS4-TLC sampler. Chromatograms

were developed in a ADC2-TLC chamber previously saturated with 2-propanol:1-butanol: acetic acid: boric acid (20 mg/mL) mixed in a ratio of 30:10:3:7 (v/v/v) used as the mobile phase. The tank saturation time was set to 45 min using a saturation pad, while the plate preconditioning time was 5 min. The relative humidity was maintained at 33%, with an activation time of 10 min and a plate drying time of 5 min. The migration distance was set to 75 mm.

To visualize the products of enzymatic decomposition of starch, the derivatization of the analytes was performed. The derivatization reagent was prepared by dissolving 2 g of diphenylamine and 2 mL of aniline in 80 mL of methanol, then adding 10 mL of phosphoric acid (85% v/v) and making up the volume to 100 mL with methanol. Derivatization was performed using an automatic TLC Derivatizer, by spraying 2 mL of reagent onto the HPTLC plate (yellow nozzle, level 6), followed by heating at 110 °C for 5 min. After cooling, the plates were photographed (TLC visualizer 2) under transmission white light.

The spectrodensitometric analysis was performed in the absorption mode at 380 and 625 nm by a TLC Scanner 4. Relative  $\alpha$ -amylase activity (%RAA<sub>TLC</sub>) was determined based on the content of maltose, maltotriose and maltotetraose, according to the equation: %RAA<sub>TLC</sub> = (PA<sub>sample</sub>/PA<sub>control</sub>) x 100, where PA<sub>sample</sub> and PA<sub>control</sub> are the sums of the products peak areas in tested and control samples, respectively. While  $\alpha$ -amylase inhibitory activity (%AIA<sub>TLC</sub>) was calculated as: %AIA<sub>TLC</sub> = 100 - %RAA<sub>TLC</sub>.

### TLC-MS analyses

Starch degradation products in post-reaction mixtures obtained after treatment with PA and AA, were identified by TLC-MS analysis according to Litewski et al. (2023)<sup>51</sup>, with minor adaptation. Briefly, samples were multi-spotted onto HPTLC plates (20 × 10 cm, Silica gel 60 F<sub>254</sub>, MS-grade, Merck, Darmstadt, Germany) and developed under the same conditions as described in HPTLC analyses section. After development and drying, only a portion of the plate was derivatized; the visible bands on the derivatized lane were used to register the position of the round elution head (4 mm) of the TLC-MS interface (CAMAG, Muttenz, Switzerland) on the non-derivatized tracks. Elution was performed with acetonitrile/water (1:1, v/v) at 0.2 mL min<sup>-1</sup> delivered by an Agilent 1200 HPLC pump. Background spectra of the silica plate were recorded and subtracted from analyte spectra.

The eluate was introduced into a Thermo Q-Exactive™ Focus quadrupole-Orbitrap high-resolution mass spectrometer (Thermo, Bremen, Germany) equipped with HESI-II source operated in negative ion mode. Source parameters were: sheath gas, auxiliary gas, and sweep gas flow rates were set to 35 arb, 15 arb, and 3 arb, respectively. The spray voltage was adjusted to 2.5 kV, with an S-lens RF level of 50. The capillary and heater temperatures were maintained at 350 °C and 300 °C, respectively. The full MS scan covered a mass range of 120–1200 *m/z*, with a resolution of 70,000 FWHM, an AGC target of 2 × 10<sup>5</sup>, and a maximum injection time of 100 ms. Data-dependent MS<sup>2</sup> used: 17,500 resolution; 3.0 *m/z* isolation window; NCE 30; AGC target 1 × 10<sup>6</sup>; automatic IT. Raw files were processed in Compound Discoverer 3.3 (Thermo Fisher Scientific, Waltham, MA, USA) and MS<sup>2</sup> ion nomenclature followed Domon & Costello (1988)<sup>31</sup>.

Identification levels and criteria. We analysed three authentic standards, maltose, maltotriose and maltotetraose, under identical HPTLC-MS conditions. These features were confirmed (Level 1) by (i) HPTLC co-migration with standards ( $\Delta Rf < 0.02$ ) and (ii) MS/MS spectral matching of diagnostic fragments. For higher malto-oligosaccharides (dp5-dp7), authentic standards were not available; therefore, assignments are reported as putative (Level 2) based on (i) accurate mass within  $\leq 5$  ppm, (ii) adduct type/isotopic fit consistent with malto-oligosaccharides, and (iii) HRMS/MS patterns characteristic for these structures.

### Method validation

The validation of the developed HPTLC method was performed for three main starch degradation products: maltose, maltotriose and maltotetraose according to the procedure described by Borman & Elder (2017)<sup>34</sup>.

### Linearity and detectability

To assess the linearity of the analytical method, HPTLC analysis was performed for aqueous solutions of three standard substances - maltose, maltotriose and maltotetraose - at concentrations ranging from 50 to 1200 ng/band, using a dosing volume of 2  $\mu$ L. For each standard, the analysis was performed in triplicate. Peak areas were quantified from the densitograms obtained and utilized to generate five-point linear calibration curves, which were subsequently evaluated through linear regression analysis. To assess the detectability, which is the ability to detect and quantify small amounts of the analyte in the sample, limit of detection (LOD) and limit of quantification (LOQ) were determined. For each standard, the LOD and LOQ parameters were calculated using the following equations: LOD = 3 x S/ $\sigma$  and LOQ = 10 x S/ $\sigma$ , where S is the slope of the calibration curve and  $\sigma$  is the standard deviation of the noise signal, which was obtained by integrating a baseline area of the same size as the analyte signal on each track.

### Accuracy

The accuracy of an analytical method reflects its ability to produce results close to the true or expected value. In this study, accuracy was assessed using the spiking (over-spotting) approach. Standard solutions were applied to the HPTLC plate at three levels (400, 600, and 800 ng/band), followed by the application of 1  $\mu$ L of 5 mg/mL soluble starch solution on top of the standards. As a control, standards were also applied without subsequent starch addition. All experiments were conducted in triplicate. The following equations were used to estimate %recovery and %relative standard deviation (RSD): %recovery = (C<sub>measured</sub> / C<sub>spiked</sub>) x 100, where C<sub>measured</sub> is the measured analyte concentration; C<sub>spiked</sub> is the analyte concentration corresponding to the respective spike level (400, 600 or 800 ng/band) and %RSD = (SD/C<sub>mean measured</sub>) x 100, where SD is the standard deviation of the measured concentrations, C<sub>mean measured</sub> is the mean value of the measured concentrations.

## Precision

The precision of an analytical procedure expresses the degree of agreement (or scatter) between a series of measurements obtained from multiple samplings of the same homogeneous sample under defined conditions. Intra-day precision was tested by analysing medium-range concentration of standards (400 ng/band;  $n=7$ ) on the same day using the developed method. For inter-day precision, standard solutions at 400 ng/band were analysed in triplicate across different days ( $n=9$ ). Precision was expressed as the percentage relative standard deviation (%RSD) of the amounts of standards determined using calibration curves for each standard.

## Statistical analysis

All data were analysed using Microsoft Excel and GraphPad Prism 10.6.0 software (GraphPad Software, Boston, MA, USA, available at <https://www.graphpad.com>), with a significance threshold set at  $p \leq 0.05$ . Unless indicated otherwise, results are expressed as mean values  $\pm$  standard deviation (SD) from at least three independent measurements. Statistical significance was assessed using one-way ANOVA followed by either the Tukey-Kramer or Dunnett's post hoc test, as appropriate. Comparisons between the HPTLC and DNS methods were additionally performed using the Student's t-test.

## Data availability

Data supporting the results presented in this study are available from the corresponding authors upon reasonable request (S.L.; [szyomon.litewski@pg.edu.pl])(mailto: szyomon.litewski@pg.edu.pl)).

Received: 25 June 2025; Accepted: 30 September 2025

Published online: 06 November 2025

## References

- Rashwan, A. K. et al. Plant starch extraction, modification, and green applications: A review. *Environ. Chem. Lett.* **22**, 2483–2530. <https://doi.org/10.1007/s10311-024-01753-z> (2024).
- Paul, J. S., Gupta, N., Beliya, E., Tiwari, S. & Jadhav, S. K. Aspects and recent trends in microbial  $\alpha$ -Amylase: a review. *Appl. Biochem. Biotechnol.* **193** (8), 2649–2698. <https://doi.org/10.1007/s12010-021-03546-4> (2021).
- de Souza, P. M. & de Magalhães, O. Application of microbial  $\alpha$ -amylase in industry - A review. *Braz J. Microbiol.* **41** (4), 850–861. <https://doi.org/10.1590/S1517-83822010000400004> (2010).
- Musdalifa, M., Laga, A. & Rahman, A. N. F. Glucose syrup production through enzymatic methods and acid hydrolysis using different starch sources: A systematic review. *Food Biophys.* **18**, 8976–8992. <https://doi.org/10.1007/s11694-024-02852-9> (2024).
- Xu, Q. S., Yan, Y. S. & Feng, J. X. Efficient hydrolysis of Raw starch and ethanol fermentation: a novel Raw starch-digesting glucoamylase from *Penicillium oxalicum*. *Biotechnol. Biofuels.* **9**, 216. <https://doi.org/10.1186/s13068-016-0636-5> (2016).
- Farooq, M. A. et al. Biosynthesis and industrial applications of  $\alpha$ -amylase: a review. *Arch. Microbiol.* **203** (4), 1281–1292. <https://doi.org/10.1007/s00203-020-02128-y> (2021).
- Proença, C., Ribeiro, D., Freitas, M. & Fernandes, E. Flavonoids as potential agents in the management of type 2 diabetes through the modulation of  $\alpha$ -amylase and  $\alpha$ -glucosidase activity: a review. *Crit. Rev. Food Sci. Nutr.* **62** (12), 3137–3207. <https://doi.org/10.1080/10408398.2020.1862755> (2022).
- Date, K., Yamazaki, T., Toyoda, Y., Hoshi, K. & Ogawa, H.  $\alpha$ -Amylase expressed in human small intestinal epithelial cells is essential for cell proliferation and differentiation. *J. Cell. Biochem.* **121** (2), 1238–1249. <https://doi.org/10.1002/jcb.29357> (2020).
- Jenkins, D. J. et al. Glycemic index: overview of implications in health and disease. *The Am J. Clin. Nutr.* **76** (1). <https://doi.org/10.1093/ajcn/76.1.266S> (2002). 266S–73S.
- International Diabetes Federation. IDF Diabetes Atlas, 11th ed.; International Diabetes Federation: Brussels. (2025). <https://diabetesatlas.org> (2025).
- Lankatillake, C., Huynh, T. & Dias, D. A. Understanding glycaemic control and current approaches for screening antidiabetic natural products from evidence-based medicinal plants. *Plant. Methods.* **15**, 105. <https://doi.org/10.1186/s13007-019-0487-8> (2019).
- Abel, E. D. et al. Diabetes mellitus-Progress and opportunities in the evolving epidemic. *Cell* **187** (15), 3789–3820. <https://doi.org/10.1016/j.cell.2024.06.029> (2024).
- Antar, S. A. et al. Diabetes mellitus: Classification, mediators, and complications; A gate to identify potential targets for the development of new effective treatments. *Biomed. Pharmacother.* **168**, 115734. <https://doi.org/10.1016/j.bioph.2023.115734> (2023).
- Tomic, D., Shaw, J. E. & Magliano, D. J. The burden and risks of emerging complications of diabetes mellitus. *Nat. Rev. Endocrinol.* **18** (9), 525–539. <https://doi.org/10.1038/s41574-022-00690-7> (2022).
- Riyaphan, J., Pham, D. C., Leong, M. K. & Weng, C. F. In Silico approaches to identify polyphenol compounds as  $\alpha$ -Glucosidase and  $\alpha$ -Amylase inhibitors against Type-II diabetes. *Biomolecules* **11** (12), 1877. <https://doi.org/10.3390/biom11121877> (2021).
- Ardalani, H., Hejazi Amiri, F., Hadipanah, A. & Kongstad, K. T. Potential antidiabetic phytochemicals in plant roots: a review of in vivo studies. *J. Diabetes Metab. Disord.* **20** (2), 1837–1854. <https://doi.org/10.1007/s40200-021-00853-9> (2021).
- Takahashi, J. A., Rezende, F. A. G. G., Moura, M. A. F., Dominguez, L. C. B. & Sande, D. Edible flowers: bioactive profile and its potential to be used in food development. *Food Res. Int.* **129**, 108868. <https://doi.org/10.1016/j.foodres.2019.108868> (2020).
- Mlcek, J. & Rop, O. Fresh edible flowers of ornamental plants - A new source of nutraceutical foods. *Trends Food Sci. Technol.* **22** (10), 561–569. <https://doi.org/10.1016/j.tifs.2011.04.006> (2011).
- Visvanathan, R. et al. Critical review on conventional spectroscopic  $\alpha$ -amylase activity detection methods: merits, demerits, and future prospects. *J. Sci. Food Agric.* **100** (7), 2836–2847. <https://doi.org/10.1002/jsfa.10315> (2020).
- Freitas, D. et al. Interlaboratory validation of an optimized protocol for measuring  $\alpha$ -amylase activity by the INFOGEST international research network. *Sci. Rep.* **15**, 30985. <https://doi.org/10.1038/s41598-025-12561-y> (2025).
- Franco, J. M., Murado, M. A., Siso, M. I. G., Miron, J. & Gonzalez, M. P. A HPLC method for specific determination of  $\alpha$ -amylase and glucoamylase in complex enzymatic preparations. *Chromatographia* **27**, 328–332. <https://doi.org/10.1007/BF02321279> (1989).
- Aranda, M. B., Vega, M. H. & Villegas, R. F. Routine method for quantification of starch by planar chromatography (HPTLC). *J. Planar Chromatogr. - Mod. TLC.* **18** (4), 285–289. <https://doi.org/10.1556/JPC.18.2005.4.6> (2005).
- Morlock, G. E. & Sabir, G. Comparison of two orthogonal liquid chromatographic methods for quantitation of sugars in food. *J. Liq. Chromatogr. Rel. Technol.* **34** (10–11), 902–919. <https://doi.org/10.1080/10826076.2011.571118> (2011).
- Islam, M. K., Sostaric, T., Lim, L. Y., Hammer, K. & Locher, C. A validated method for the quantitative determination of sugars in honey using high-performance thin-layer chromatography. *JPC - J. Planar Chromat.* **33**, 489–499. <https://doi.org/10.1007/s00764-020-00054-9> (2020).

25. Schwack, W., Heilmann, D. & Morlock, G. E. Ethylamine as a new derivatization reagent differentiating reducing from non-reducing saccharides. *J. Planar Chromatogr. - Mod. TLC*. **36**, 359–366. <https://doi.org/10.1007/s00764-023-00266-9> (2023).
25. Müller, I. & Morlock, G. E. Quantitative saccharide release of hydrothermally treated flours by validated salivary/pancreatic on-surface amylolysis (nanoGIT) and high-performance thin-layer chromatography. *Food Chem.* **432**, 137145. <https://doi.org/10.1016/j.foodchem.2023.137145> (2024).
27. Müller, I., Schmid, B., Bosa, L. & Morlock, G. E. Screening of  $\alpha$ -amylase/trypsin inhibitor activity in wheat, spelt and Einkorn by high-performance thin-layer chromatography. *Anal. Methods.* **16** (19), 2997–3006. <https://doi.org/10.1039/d4ay00402g> (2024).
28. Litewski, S., Koss-Mikolajczyk, I. & Kusznierewicz, B. Comparative analysis of phytochemical profiles and selected biological activities of various morphological parts of *ligustrum vulgare*. *Molecules* **29** (2), 399. <https://doi.org/10.3390/molecules29020399> (2024).
29. Miller, G. L. Use of Dinitrosalicylic acid reagent for determination of reducing sugar. *Anal. Chem.* **31**, 426–428. <https://doi.org/10.1021/ac60147a030> (1959).
30. Yi, L. et al. UP-HILIC-MS/MS to determine the action pattern of *penicillium* sp. Dextranase. *J. Am. Soc. Mass. Spectrom.* **26** (7), 1174–1185. <https://doi.org/10.1007/s13361-015-1117-y> (2015).
31. Domon, B. & Costello, C. E. A systematic nomenclature for carbohydrate fragmentations in FAB-MS/MS spectra of glycoconjugates. *Glycoconj. J.* **5**, 397–409. <https://doi.org/10.1007/BF01049915> (1988).
32. Butterworth, P. J., Warren, F. J. & Ellis, P. R. Human  $\alpha$ -amylase and starch digestion: an interesting marriage. *Starch-Stärke* **63** (7), 395–405. <https://doi.org/10.1002/star.201000150> (2011).
33. Sahnoun, M. et al. Production purification and characterization of two  $\alpha$ -amylase isoforms from a newly isolated *Aspergillus oryzae* strain S2. *Process. Biochem.* **47**, 18–25. <https://doi.org/10.1016/j.procbio.2011.09.016> (2011).
34. Borman, P. J. & Elder, D. P. Q2(R1) validation of analytical procedures: text and methodology. *Chapter 5 ICH Qual. Guide Implement. Guide.* **127-166** <https://doi.org/10.1002/9781118971147.ch5> (2017). (Wiley, 2017).
35. Mello dos Santos, M., Jacobs, C., Islam, M. K., Lim, L. Y. & Locher, C. Validation of a high-performance thin-layer chromatography method for the quantitative determination of trehalulose. *J. Planar Chromatogr. - Mod. TLC*. **36**, 201–210. <https://doi.org/10.1007/s00764-023-00243-2> (2023).
36. Zheng, J., Lu, B. & Xu, B. An update on the health benefits promoted by edible flowers and involved mechanisms. *Food Chem.* **340**, 127940. <https://doi.org/10.1016/j.foodchem.2020.127940> (2021).
37. Brglez Mojzer, E., Knez Hrnčič, M., Škerget, M., Knez, Ž. & Bren, U. Polyphenols: extraction Methods, antioxidative Action, bioavailability and anticarcinogenic effects. *Molecules* **21** (7), 901. <https://doi.org/10.3390/molecules21070901> (2016).
38. Mróz, M., Malinowska-Pańczyk, E., Bartoszek, A. & Kusznierewicz, B. Comparative study on assisted solvent extraction techniques for the extraction of biologically active compounds from *Sideritis raeseri* and *Sideritis Scardica*. *Molecules* **28** (10), 4207. <https://doi.org/10.3390/molecules28104207> (2023).
39. Deshavath, N. N., Mukherjee, G., Goud, V. V., Veeranki, V. D. & Sastry, C. V. Pitfalls in the 3, 5-dinitrosalicylic acid (DNS) assay for the reducing sugars: interference of furfural and 5-hydroxymethylfurfural. *Int. J. Biol. Macromol.* **156**, 180–185. <https://doi.org/10.1016/j.ijbiomac.2020.04.045> (2020).
40. Thakur, M. et al. Hypoglycemic and antioxidant activities of *Jasminum officinale* L. with identification and characterization of phytocompounds. *Helijon* **10** (21), e39165. <https://doi.org/10.1016/j.helijon.2024.e39165> (2024).
41. Zengin, G. et al. Chemical profiling of *Centaurea bornmuelleri* Haussk. Aerial parts by HPLC-MS/MS and their pharmaceutical effects: from nature to novel perspectives. *J. Pharm. Biomed. Anal.* **174**, 406–413. <https://doi.org/10.1016/j.jpba.2019.06.009> (2019).
42. Tang, S. R. et al. Phenolic compounds from *Gomphrena globosa* L.: phytochemical analysis, antioxidant, antimicrobial, and enzyme inhibitory activities in vitro. *CyTA - J. Food.* **20** (1), 218–227. <https://doi.org/10.1080/19476337.2022.2125584> (2022).
43. Nowicka, P. & Wojdylo, A. Anti-Hyperglycemic and anticholinergic effects of natural antioxidant contents in edible flowers. *Antioxidants* **8** (8), 308. <https://doi.org/10.3390/antiox8080308> (2019).
44. Jaradat, N. et al. Phytochemical composition and antidiabetic, anti-obesity, antioxidant, and cytotoxic activities of *Carthamus tinctorius* seed oil. *Sci. Rep.* **14**, 31399. <https://doi.org/10.1038/s41598-024-83008-z> (2024).
45. Cucu, A. A. et al. *Calluna vulgaris* as a Valuable Source of Bioactive Compounds: Exploring Its Phytochemical Profile, Biological Activities and Apitherapeutic Potential. *Plants.* **11**(15), ; (1993). <https://doi.org/10.3390/plants11151993> (2022).
46. Dienaité, L. et al. Isolation of strong antioxidants from *Paeonia officinalis* roots and leaves and evaluation of their bioactivities. *Antioxidants* **8** (8), 249. <https://doi.org/10.3390/antiox8080249> (2019).
47. Zhang, C. C., Geng, C. A., Huang, X. Y., Zhang, X. M. & Chen, J. J. Antidiabetic Stilbenes from peony seeds with PTP1B,  $\alpha$ -Glucosidase, and DPPIV inhibitory activities. *J. Agric. Food Chem.* **67** (24), 6765–6772. <https://doi.org/10.1021/acs.jafc.9b01193> (2019).
48. Simin, N. et al. New garden Rose (*Rosa × hybrida*) genotypes with intensely colored flowers as rich sources of bioactive compounds. *Plants* **13** (3), 424. <https://doi.org/10.3390/plants13030424> (2024).
49. Qiu, L., Zhang, M., Mujumdar, A. S. & Chang, L. Effect of edible Rose (*Rosa rugosa* cv. Plena) flower extract addition on the physicochemical, rheological, functional, and sensory properties of set-type yogurt. *Food Biosci.* **42**, 101179. <https://doi.org/10.1016/j.fbio.2021.101179> (2021).
50. Gonçalves, C., Rodriguez-Jasso, R. M., Gomes, N., Teixeira, J. A. & Belo, I. Adaptation of Dinitrosalicylic acid method to microtiter plates. *Anal. Methods.* **2** (12), 2046–2048. <https://doi.org/10.1039/C0AY00525H> (2010).
51. Litewski, S., Mróz, M., Bartoszek, A. & Kusznierewicz, B. Post-Chromatographic derivatization coupled with mass spectrometry as a method of profiling and identification of Antioxidants; *Ligustrum vulgare* phytocomplex as an example. *Molecules* **28** (24), 8000. <https://doi.org/10.3390/molecules28248000> (2023).

## Author contributions

S. Litewski: Formal analysis, Investigation, Methodology, Validation, Writing - original draft; M. Mróz: Investigation, Methodology, Writing - review and editing; B. Kusznierewicz: Conceptualization, Formal analysis, Funding acquisition, Methodology, Project administration, Resources, Supervision, Visualization, Writing - review and editing.

## Funding sources

This research did not receive any specific grant from funding agencies in the public, commercial, or not-for-profit sectors.

## Declarations

### Competing interests

The authors declare no competing interests.

### Additional information

Correspondence and requests for materials should be addressed to S.L. or B.K.

Reprints and permissions information is available at [www.nature.com/reprints](http://www.nature.com/reprints).

**Publisher's note** Springer Nature remains neutral with regard to jurisdictional claims in published maps and institutional affiliations.

**Open Access** This article is licensed under a Creative Commons Attribution-NonCommercial-NoDerivatives 4.0 International License, which permits any non-commercial use, sharing, distribution and reproduction in any medium or format, as long as you give appropriate credit to the original author(s) and the source, provide a link to the Creative Commons licence, and indicate if you modified the licensed material. You do not have permission under this licence to share adapted material derived from this article or parts of it. The images or other third party material in this article are included in the article's Creative Commons licence, unless indicated otherwise in a credit line to the material. If material is not included in the article's Creative Commons licence and your intended use is not permitted by statutory regulation or exceeds the permitted use, you will need to obtain permission directly from the copyright holder. To view a copy of this licence, visit <http://creativecommons.org/licenses/by-nc-nd/4.0/>.

© The Author(s) 2025